Academia Journal of Scientific Research 7(8): 000-000, August 2019
DOI: 10.15413/ajsr.2019.0208
ISSN 2315-7712

Academia Publishing

Research Paper

A unified enhancement approach for the hazy aerial images based on the imaging physical model

Accepted 30th August, 2019

Wei Sun and Jie Huang

School of Aerospace Science and Technology, Xidian University, No.2 South Tabai Rd., Xi'an, Shaanxi, 710071, China.

*Corresponding author. E-mail: wsun@xidian.edu.cn.

ABSTRACT

This article proposes a unified method which skillfully provides a cohesive solution for non-uniform illumination and hazy aerial images based on atmospheric scattering model. The minimum RGB component of each pixel which is defined as hazy veil using the fast joint bilateral filter was first acquired followed by the scene illumination veil from the proposed residual RGB components of each pixel. Based on the residual RGB components, the RGB reflectivity per pixel can be calculated using the imaging physical model. Moreover, the proposed method uses the hazy image model for image enhancement and as such does not require evaluation of the global atmospheric light. Experimental results of various outdoor dark and hazy images indicated that the presented approach has made a good recovery in visibility and color fidelity. It gets a better balance of objective valuation between contrast, edges and color.

Key words: Aerial image dehazing, dark channel precedent, scene illumination, illumination veil, image quality assessment.

INTRODUCTION

Acquired images lose the brightness of the subject and its color clarity due to hazy weather, often caused by suspended particles in the air. The image dehazing techniques with the capability of increasing visibility and correcting color shift has played an increasing crucial role in the computer vision applications, the targets detection and tracking. In the last few years, considerable attention was paid to the haze elimination methods based on the atmospheric scattering model. Most of these studies took the scene depth information from hazy image as a significant clue for haze elimination. Schechner et al. (2003) and Narasimhan and Nayar (2002) recovered the depth information by means of the polarized light in disparate directions. However, it is very hard to get depth information from a single hazy image, while getting satisfactory dehazy results from multiple images remain an open problem to be solved.

Meanwhile, the research concerning single image dehazing is recently becoming popular, which is a bad negative matter with constraints. Correspondingly, in order to surmount the limitations of plural image dehazing methods, several single image dehazing algorithms which utilize strict restriction to eliminate the fog in a single picture have been developed (Schechner et al., 2003; Narasimhan and Nayar, 2002; Garg and Nayar, 2007). Tan and Oakley (2008) assumed that to maximize the contrast of the hazy image no haze image contrast is higher than the hazy image. In addition, this kind of method produces heavy ring effect. Fattal (2008) recovered the hazy images by disintegrating the scene radiation of an image. However, this method can only remove the haze partially but cannot recover the dense hazy scene. Kopf et al. (2008) proposed a method for the three-dimensional model of the scene, but this depends on the environment and needs additional information. Tarel and Hautiere (2009) put forward a visual recovery algorithm but there were several parameters that could not be trimmed. He proposed the method of estimating atmospheric veil by dark channel (He

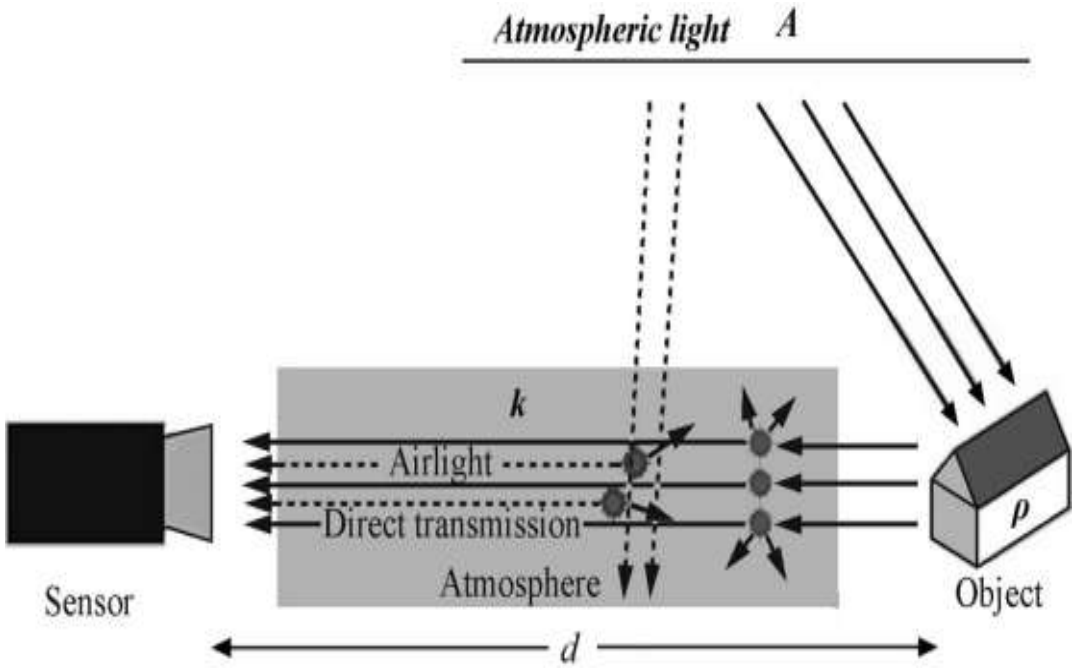

Figure 1: Atmospheric scattering model.

et al., 2009) aiming at the precedent of dark channel prior, and refining it with soft matting of heavy computing. Ancuti et al. (2011) and several other researchers, Kim et al. (2013), Tripathi and Mukhopadhyay (2012), Narasimhan and Nayar (2003) and Tan (2008) worked on He's algorithm and made it better. However, there are still some problems to be addressed.

The experiments show that the global light atmosphere in the optical imaging model which is a very significant parameter for the brightness of the restored image can be figured out by the light intensity of an infinite point (Wei and Guo, 2013; Wei, 2013). However, the researchers still do not find an accurate method to calculate the global atmospheric light at present (Yeh et al., 2013). As a result, the halos will inevitably appear in some regions of the restored images. Therefore, our research aims at a novel image dehazing method without global atmospheric light estimation.

This article proposes a novel dehazing algorithm for outdoor images and a method based on the atmospheric scattering model. The approach is in the view of the statistics. Among the surface reflectance coefficients of R, G, and B components for each point on the vivid colorful objects, the smallest is close to 0 and the largest is close to 1 (Sun et al., 2014). The hazy imagine can be enhanced by the following procedures. Firstly, the minimum intensity of RGB components which is defined as the initial atmospheric veil is calculated. At the same time, the residual image is achieved by subtracting the initial atmospheric veil from the hazy image. Secondly, the maximum magnitude of RGB components is calculated from the residual image which is defined as the scene illumination veil of the image. The atmospheric and illumination veils are further refined by the cross bilateral filtering algorithm. Finally, each RGB reflectance component can be figured out using the optical imaging model. The method in this paper has two advantages. Hazy images can be enhanced without figuring out the global atmosphere. In addition, the reflectance of RGB channels of the hazy images can also be restored and the visibility and color accurately improved.

PREVIOUS RELATED WORKS

Background Research of He's Algorithm

The imaging model widely used in the fogy image systems is given by Koschmieder. This is depicted shown in Equation (1) and Figure (1). Equation (1) is given as:

$$L(a,b) = L_0(a,b)e^{-kd(a,b)} + A(1-e^{-kd(a,b)}) \quad (1)$$

In Equation 1), $L(a,b)$ is the hazy image, while $L_0(a,b)$ is

the original image. $d(a,b)$ is the range of the homologous pixel. A is a constant defined as global atmospheric light and k is the atmosphere scattering coefficient. Through assuming a linear response camera, this model can directly be extended to color images based on the RGB model.

According to the Equation (1) and illumination-reflectance model, $L_0(a,b)$ can be rewritten as:

$$L_0(a,b) = I_0(a,b)\rho(a,b) \tag{2}$$

Where $I_0(a,b)$ is defined as illumination veil and $\rho(a,b)$ as the reflection coefficient of the scene. According to Equation (1), the goal of dehazing is to restore L_0 from L. For an N-pixel color image L, there are $3N$ constraints and $4N+3$ unknowns. L_0 has $3N$ unknowns,while $t = e^{-kd(a,b)}$ has N unknowns and A has 3 unknowns. These unknowns will cause the ill-posed matter of dehazing. The state-of-art algorithms for hazy removal focus on the inference of atmosphere veil is $V(a,b) = A(1-e^{-kd(a,b)})$ from $L(a,b)$.

According to the dark channel precedent previously (He et al., 2009; Wei and Guo, 2013; Wei, 2013), the lowest reflectivity among the RGB channels for point (a,b) in a color image $L(a,b)$ is mostly defined as $\rho(a,b) \to 0$. In the presence of the white haze, the atmosphere veil can be figured out for each point as shown in Equation (3):

$$V(a,b) = A(1-e^{-kd(a,b)}) = \lim_{\rho(a,b)\to 0} L(a,b) \tag{3}$$

Assuming $d(a,b) \to \infty$, we have:

$$A = \lim_{d(a,b)\to\infty} V(a,b) \tag{4}$$

As a result, given $\rho(a,b) \to 0$ and $d(a,b) \to \infty$, $V(a,b)$, A, and $e^{-kd(a,b)}$ can be calculated. $L_0(a,b)$ can be further figured out by Equation (1). With the white haze premise, $V(a,b)$ changes with (a,b) and A is identical for all RGB channels.

In this paper, Equations (3) and (4) are joint for solving $L_0(a,b)$. However, the structure of the real scene is very complex. In addition, the condition that $\rho(a,b) \to 0$ will not be satisfied at every pixel and even the assumption of $d(a,b) \to \infty$ cannot also be guaranteed in every image. Therefore, a filtering algorithm should be proposed to get an accurate value of A and $V(a,b)$. In the report of Asmuni et al. (2013), $V(a,b)$ defined as the dark channel by He et al. (2009) is first estimated by Equation (5) given as:

$$V_{dc}(a,b) = \min_{c\in\{R,G,B\}} L_c(a,b) \tag{5}$$

The global atmospheric light A in Equation (1) is often approximated by the intensity of brightest pixel. Xiao and Gan (2012) used the dark channel to enhance the accuracy of the estimation value of the atmospheric light. The brightest pixel (0.2%) in the dark channel was first selected, followed by the specific brightest pixel value as the global atmospheric light A. However, the scheme presented by Xiao may result in undesirable estimation of global atmospheric light because the brightest pixels of white scene in image maybe brighter than the global atmospheric light value. Meanwhile, Wei and Guo (2013) in their report stated that the halo effect will be produced in the dehazing images.

FOG REMOVAL BASED ON DARK CHANNEL AND ILLUMINATION COMPENSATION

Crux idea of the presented dehazing approach

In order to restore the true appearance of the target, the reflection coefficient $\rho(a,b)$ of the target which is an important parameter to improve the brightness and contrast of the image should be calculated. The proposed method also has the advantage of avoiding the risks caused by error of the global atmosphere light A.

From Equations (1) and (3), the residual image $L_s(a,b)$ without atmospheric veil can be obtained:

$$L_s(a,b) = L(a,b) - V(a,b) = L_0(a,b)e^{-kd(a,b)} \tag{6}$$

By combining the results of Equations (2) and (6), Equation (7) can be obtained:

$$L_s(a,b) = [I_0(a,b)e^{-kd(a,b)}]\rho(a,b) \tag{7}$$

In accordance with the imaging model in Equation (2), we

take $I(a,b)=[I_0(a,b)e^{-kd(a,b)}]$ as the scene illumination function. The dehazing method is resolved by calculating the reflection coefficient from the residual image through illumination compensation as shown in Equation (8):

$$\rho(a,b)=L_s(a,b)/[I_0(a,b)e^{-kd(a,b)}] \tag{8}$$

Actually, the reflectance is a desirable feature for computer vision to restore reflectance from color images. Many algorithms have been developed for this, including several famous Retinex algorithms (Rahman et al., 2004; Asmuni et al., 2013; Chao, 2012; Hashemi, 2010; Seo et al., 2018; Dominik, 2017; Li et al., 2017; Ye et al., 2018; Ma et al., 2018). The algorithms have the advantages of constant color and fast processing speed, but they also have some disadvantages such as poor brightness image processing effect in dehazing.

This study assumes that the camera has a linear response to environment luminance and that the maximum response is caused by a perfect reflection which is defined by $\rho(a,b)\to 1$. In accordance with the illumination-reflectance model in Equation (2), $Ls_{r,g,b}(a,b)=I(a,b)*\rho_{r,g,b}(a,b)$ can be obtained, where $\rho_{r,g,b}(a,b)$ denotes the reflection coefficient of RGB component in position (a,b) of the target. Given $\max(\rho_{r,g,b}(a,b))\to 1$, Equation (7) for each RGB channel c can then be written as:

$$I^c(a,b)=\lim_{\rho(a,b)\to 1} L^c{}_s(a,b) \tag{9}$$

Although the condition that $\max(\rho_{r,g,b}(a,b))\to 1$ cannot be met at every pixel, there must be at least one of components R, G or B that are close to the total reflection for a small patch in the color image. Its reflectance coefficient approximately equals 1. Therefore, the illumination of this patch can be defined as the maximum of R, G and B discreteness, as is depicted in the max-RGB algorithm (Sun et al., 2014). The patch can be as small as one pixel with the proposed joint bilateral filter. The largest RGB component at pixel (a,b) in $L_s(a,b)$ can be figured out. $I(a,b)$ can be preliminarily calculated by:

$$I_{mc}(a,b)=\max_{c\in\{R,G,B\}} L^c{}_s(a,b) \tag{10}$$

A joint filtering algorithm is presented to improve the computational accuracy $I(a,b)$ from a small patch because the assumption $\max(\rho_{r,g,b}(a,b))\to 1$ cannot be met at every pixel.

From Equations (6) and (8), $\rho(a,b)$ can be figured out using atmospheric veil $V(a,b)$ and illumination veil $I(a,b)$. Obviously, it is not necessary to calculate the global atmospheric light *A* in Equation (1) in the presented approach. Therefore, the risk of calculation error in *A* can be reduced.

Atmosphere veil inference

We can have an initial estimation of $V_{dc}(a,b)$ from Equation (5), as shown in Figure 2b. According to Equation (6), a fine distribution of the atmosphere veil $V(a,b)$, which should be able to maintain the object details is required (He et al., 2010). For general smoothing, the uniform or the Gaussian kernel works very well except the smoothed edges. Bilateral filtering can be utilized to keep edge smoothing (Bai et al., 2012). Joint/cross bilateral filter smooth one source using the similarity of the other source. Its kernel is a combination of weights of the edge and the intensity similarity.

By grayscale opening morphological filtering on $V_{dc}(a,b)$, we get $V'_{dc}(a,b)$ as shown in Figure 2c. The radius of structuring element depends on the size of the object to be eliminated. Typically, we define it as r = min[w,h]/10, where w and h are the width and height of the fogy image, respectively. The morphological filtering can smooth the gray scale and remove the specific white object. However, it will result in blurred edges. We want to keep the edges of $V_{dc}(a,b)$ and the intensity values are consistent after filtering. Therefore, combined bilateral filter may be the best choice for this application. As an edge-preserving filter, with the increase in the pixel position (spatial domain S) and the gray intensity (range R), the filtering weight decreases gradually.

Given $E=V_{dc}(a,b)$, $D=V'_{dc}(a,b)$ as input data, V(a, b) is the filtered pixels by the spatial-range kernel (Figure 2d). Using the Gaussian function, Gσ for the decrement functions and the grayscale images, E and D, $p=(a,b)$, $q=\{(a,b),(a,b)\in S\}$, the filtered data of V(p) is

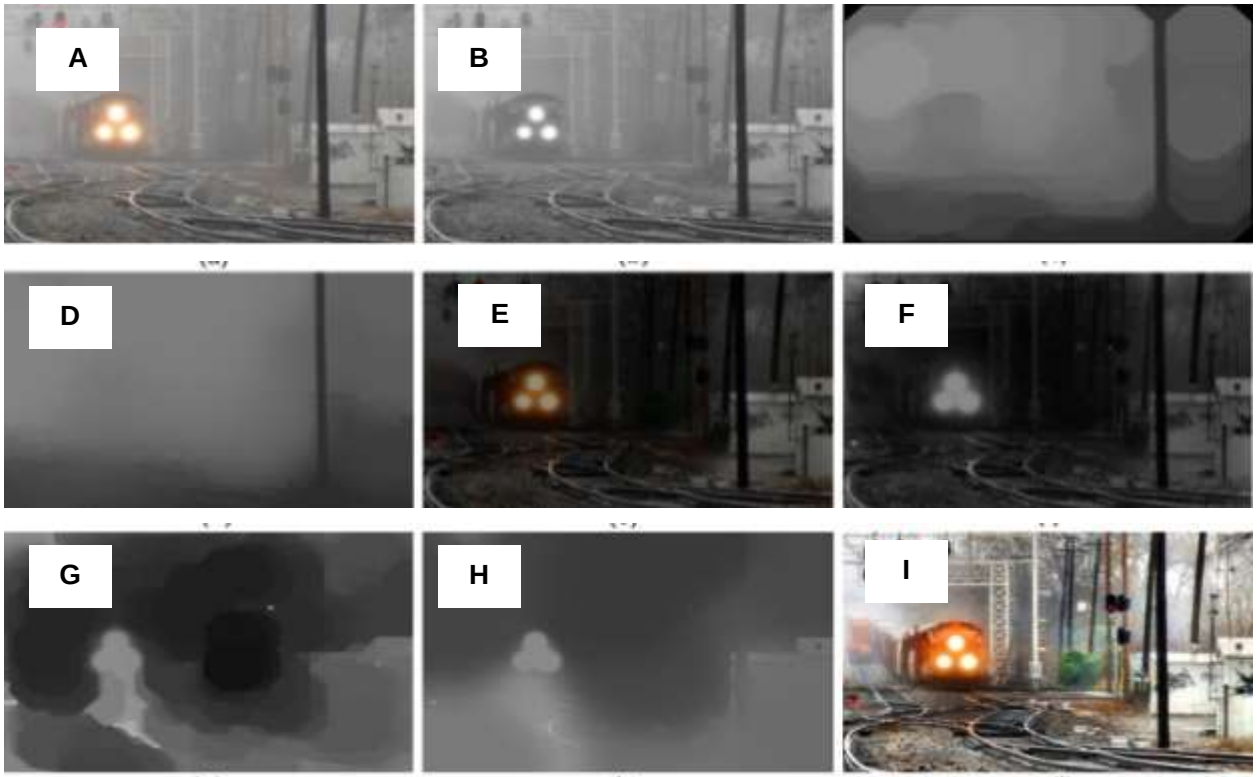

Figure 2: Restored image 'train' by the proposed algorithm. (a) Hazy image (b) Dark channel of hazy image (c) Gray opening of dark channel (d) Atmosphere veil $V(x,y)$ of the input image (e) Result of the residual image $L_s(x,y)$ (f) Max intensity of residual image (g)Gray closing of max intensity (h)Illumination veil $I(x,y)$ of the residual image $L_s(x,y)$ (i) Restored image $\rho(x,y)$ by the proposed method.

assigned through:

$$V(p)=\frac{1}{W_p}\sum_{q\in S}G_{\sigma(s)}\left(\|p-q\|\right)G_{\sigma(r)}\left(\left|E_p-E_q\right|\right)D_q \tag{11a}$$

$$W_p=\sum_{q\in S}G_{\sigma(s)}\left(\|p-q\|\right)G_{\sigma(r)}\left(\left|E_p-E_q\right|\right) \tag{11b}$$

Where $\sigma(s)$ is defined as the range of spatial neighborhood range of filtered pixels. $\sigma(r)$ controls weighting degree of adjacent pixels caused by different intensities, while W_p normalizes the sum of the weights.

The weight G_s, G_r decreases as its position and range increase.

Computation of the filtering algorithm in accordance with Equation (11) is time-consuming on account of the non-linearity filtering. Therefore, it is difficult to select the scale of Gaussian filter kernel. Paris et al. (2006) showed a fast joint filtering algorithm and discussed the numerical approximation accuracy. He defined the filter as a linear shift invariant convolution in 3-Dimension space, which resulted in a low-pass filtering in the down-sampling space. The high resolution image and the final bilateral filtering result are obtained by linear interpolation. In the research, the fast algorithm of bilateral filtering, which not only keeps the simplicity of calculation but also shows the best accuracy is used. $\sigma(s)$ and $\sigma(r)$ specifies the standard deviation of the space and range Gaussians, respectively, while $\sigma(s)$ defaults to min(^{w,h}) / 16 and $\sigma(r)$ defaults to (edgeMax - edgeMin) / 10; edgeMin and edgeMax specifies the minimun and maximum intensity of edge image input.

Illumination veil resolving

For the real scene, the illumination typically changes slowly

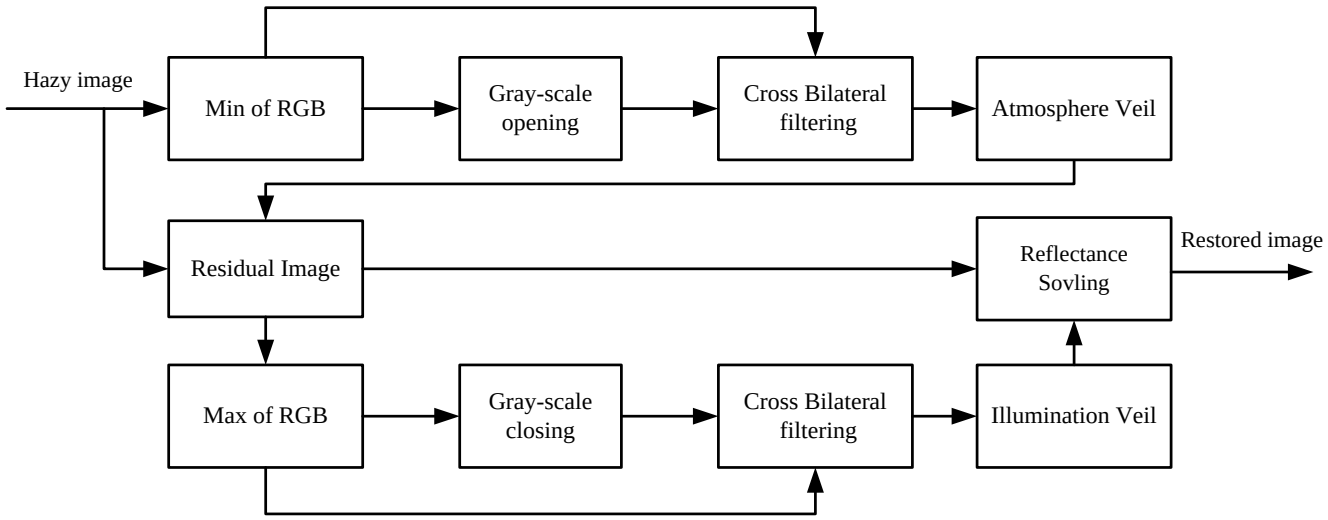

Figure 3: Block diagram of proposed dehazing algorithm for color images.

in the image, while the reflectance coefficients of the scene changes rapidly (Chao, 2012; Hashemi, 2010). As shown in Equation (7), the low-pass filtering or center/surround retinex is not the best way to remove the lighting effect of the objects in an image.

According to Equation (7), to get the restored images in Equation (8), the illumination veil function $I(a,b)$ should be calculated. As earlier mentioned the basic character of lighting $I(a,b)$ is relatively smooth in a local patch and should keep the details of the scene (Zhang et al., 2008). Similar with the solution for $V(a,b)$ earlier discussed, the cross bilateral filter matches well with the problem earlier highlighted. Therefore, a new algorithm was proposed to get $I(a,b)$, which directly calculates a better estimation of the illumination veil of the $L_s(a,b)$ as depicted in Figure 2e and Equation (7).

In this study, the morphological closing filtering on the $I_{mc}(a,b)$ as given in Figure 2f was used. The scale of the structuring element is a significant parameter to determine the brightness of the restored images, which is usually defined as $r = \min[w,h]/10$. It is adjusted dynamically. If right empirical parameters are used, the objects without vivid color can be eliminated. The morphological closing filtering result $I_{mc}(a,b)$ is defined as $I'_{mc}(a,b)$ as given in Figure 2g.

For Equation (11), $E = I_{mc}(a,b)$, $D = I'_{mc}(a,b)$, filtered data at spacial position (a,b) has the range constrain of the point in $I'_{\max}(a,b)$. $I(a,b)$ given in Figure 2h.

Scene reflectance restoration

Procedures of the presented method are given as:

1) Give the hazy color picture $L(a,b)$ with RGB model;
2) For components R, G, and B per pixel, calculate the atmosphere veil $V_{dc}(a,b)$ with Equation (5);
3) Refine $V(a,b)$ by joint bilateral filtering algorithm with $V_{dc}(a,b)$ and $V'_{dc}(a,b)$;
4) Subtract $V(a,b)$ from $L(a,b)$ to figure out the residual value $L_s(a,b)$;
5) For R, G, and B components per pixel in $L_s(a,b)$, calculate the lighting veil $I(a,b)$ using Equation (10);
6) Extract $I(a,b)$ utilizing joint bilateral filtering on $I_{mc}(a,b)$ and $I'_{mc}(a,b)$;
7) Get $\rho(a,b)$ of the objective using $L_s(a,b)/I(a,b)$ as in Equation (8) and normalize to [0 1].

In Figure 2i, the halos and blocking effects are restrained, while the dehaze image is clear and brighter than that given by He et al. (2009). As earlier mentioned, the flow chart of the presented algorithm is demonstrated in Figure 3.

Figure 4: Experiments results of image 'aerial' (a) Hazy image (b) Recovered with Rahman's algorithm(c) Recovered with He's algorithm; (d) Recovered with presented approach.

Figure 5: Experiments results of image 'people' (a) Fogy image (b) Recovered with Rahman's algorithm(c) Recovered with He's algorithm; (d) Recovered with presented approach;

EXPERIMENTS

In order to prove the performance of the proposed dehazing algorithm, several groups of typical hazy images were selected for restoration experiments, and partially shadowed images included.

Subjective evaluation

It is the ultimate goal to increase the visibility and preserve the details of the image for the image restoration algorithm. In the following experiments, an efficient filtering process calculation algorithm (Paris et al., 2006; Zhang et al., 2008) whose complexity is linearly related to the size of the image was utilized. It approximately takes 1.42 s to deal with a 735 *492 image on a PC with a CPU of 3.0 GHz Intel Pentium 4 Processor using the MATLAB 7.8.0.

The joint cross filtering was utilized to automatically estimate the atmospheric veil and illumination veil for all images shown in this study. Figures 4 and 5 demonstrate the experimental results of some outdoor hazy scenes. As can be shown, Rahman's method will cause color cast, while for the proposed method, even in the areas of dense fog and darkness, it is easy to show details and restore vivid colors. For He's restored results, it seems natural but distortion exists. For the restored image of 'aerial', the right up corner which may be caused by over- saturated pixels becomes white. When checked in detail, it was noticed that some small structures in the shadow are blurred in Figure 4c, but were kept in recovered images as given in Figure 4d. Figure 5 shows the satisfied results.

In order to give more explanations of the presented approach, another experiment was given to support our opinion. In Figure 6, comparing with He's approach based on dark channel precedent, the restored image by the proposed method presents more vivid color and seems more clear. It can be seen that the skirt pattern and color on the middle puppet are very clear. Therefore, the normalized reflection coefficient of the restored image looks like the original color image magnification. As a result, we can get more information and details in the restored image of the scene.

Figure 7 shows more experiments to support the proposed method. The M100 four-axis aircraft in DJI was used to collect actual video images. The comparable results

Figure 6: Experiments results of image 'toys' ' (a) Fogy image (b) Recovered with He's algorithm; (d) Recovered with presented approach.

Figure 7: Comparable results of hazy images(a-d) and recovered images(e-h)by proposed approach.

of hazy images (a-d) and recovered images (e-h) through the proposed approach are shown. It can be seen that the restored images are rich in color and clear in details.

Subjective and objective evaluation

In this paper, we use an approach proposed by Hautière (2008). The method defines the ratio e between the quantities of new visible edges whose local contrast between the hazy image and the one restored is above 5%. The average gradient ratio ($\overline{r}$) is defined as the objective criterion of restored images. They are given as:

$$e = \frac{n_r - n_0}{n_0} \quad \overline{r} = \frac{\overline{g}_r}{\overline{g}_0} \tag{12}$$

Where n_0 and n_r are the quantities of visible edges in the hazy image $L(x, y)$ and the restored one. $\overline{g}_r$ is the average gradient of the hazy image and $\overline{g}_0$ denotes the gradient of the restored one, while Σ is the fraction of pixels which are completely black or white after restoration.

The goal of dehazing algorithm increases the contrast without saturation and does not losing the important visual information at the same time. Contrast defines how gray levels q, q = 0, 1, ..., $q_{\max}$, vary in the image g and their distribution. The second-order of the grey level histogram (empirical probability distribution) is defined as variance, σ^2, while normalized fourth-order central moments is defined as kurtosis α_4, used to define the contrast F_{con} :

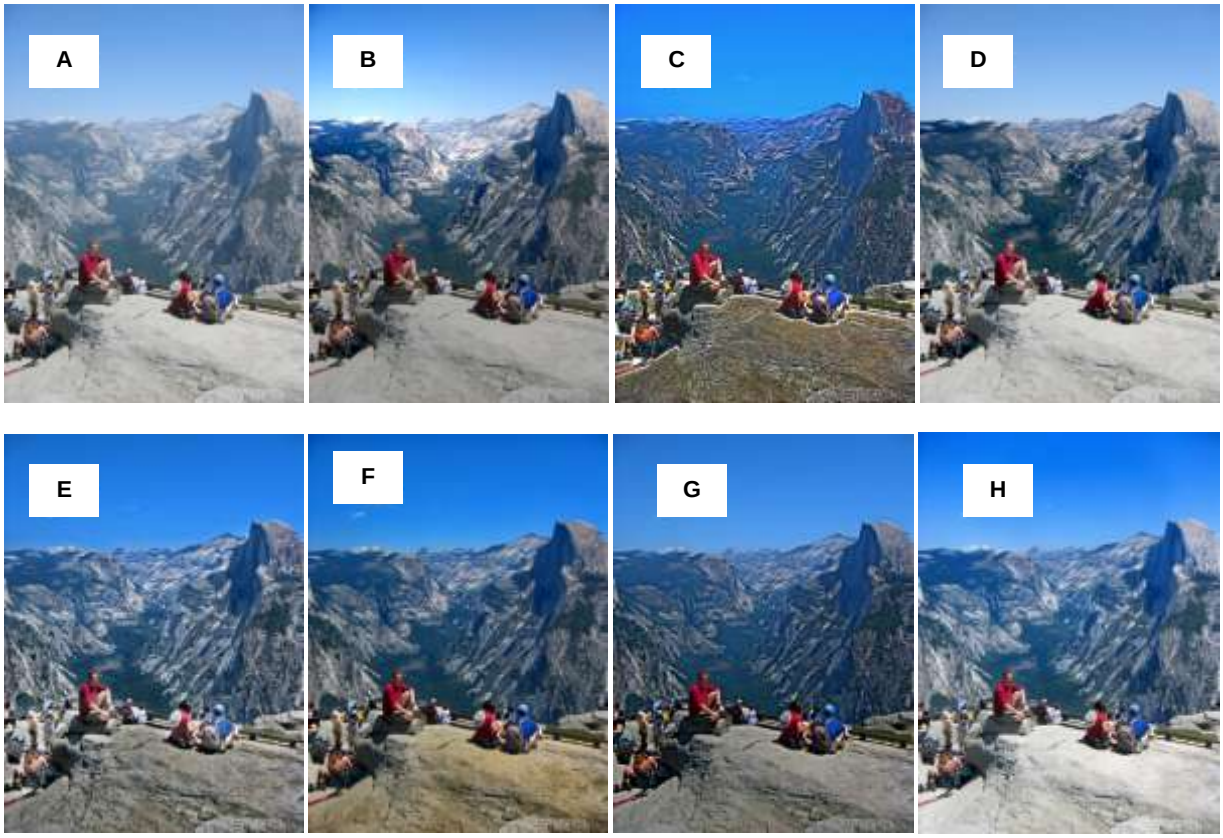

Figure 8: Comparison of qualitative performance with different algorithms of 'y16' (a) Original fogy image. (b) Fattal et al.'s method. (c) Tan et al.'s method. (d) Koef et al.'s method. (e) Tarel et al.'s method. (f)He et al.'s method. (g) A.K. et al.' method. (h) Presented method.

$$F_{con} = \frac{\delta}{\alpha_4^n} \tag{13a}$$

With:

$$\alpha_4 = \frac{\mu_4}{\sigma^4}, \quad \delta^2 = \sum_{q=0}^{q_{max}} (q-m)^2 \Pr(q \mid g), \quad \mu_4 = \sum_{q=0}^{q_{max}} (q-m)^4 \Pr(q \mid g) \tag{13b}$$

Where, m is the first order moment of the intensity probability distribution. The empirical value n=0.25 is used for discriminating the textures.

In this study, we define C_{gain} as the contrast ration between the restored and the hazy image. Large values of e, $\bar{r}$, C_{gain} and small values of Σ indicate a better algorithm performance. After subjective evaluation on color and visible details, we thereafter calculated four indicators e, $\bar{r}$, Σ and C_{gain} from the intensity of the hazy and the restored images to quantitatively evaluate the quality of the restored images and rate some proposed algorithms. All experiments were done using MATLAB 7.8.0.

Some results of multifarious hazy images: 'y01', 'y16', and 'ny17' are demonstrated in Figures 8 to 10. For Fattal's algorithm, the haze of the image was not eliminated and the details are not rich enough. Figures 9 and 10 shows the halo artifacts cannot be eliminated in Tan's method and the edge of the image is also prominent. In addition, the color is distorted. For Koef's method, the restored result is colorful and mist-free. However, the details of the image are not rich enough, and the smallest white clouds in the distant sky are not recovered. For Tarel's approach, there are also some halos artifacts and color cast. In Figures 9 and 10, He's algorithm makes the image look washed. Figure 10 shows the clouds behind the mountains have a high glow effect. For A.K's algorithm, the contrast of image is good. However, the mist removal is not clean and the details are slightly lacking. Figure 9 shows the results of the proposed

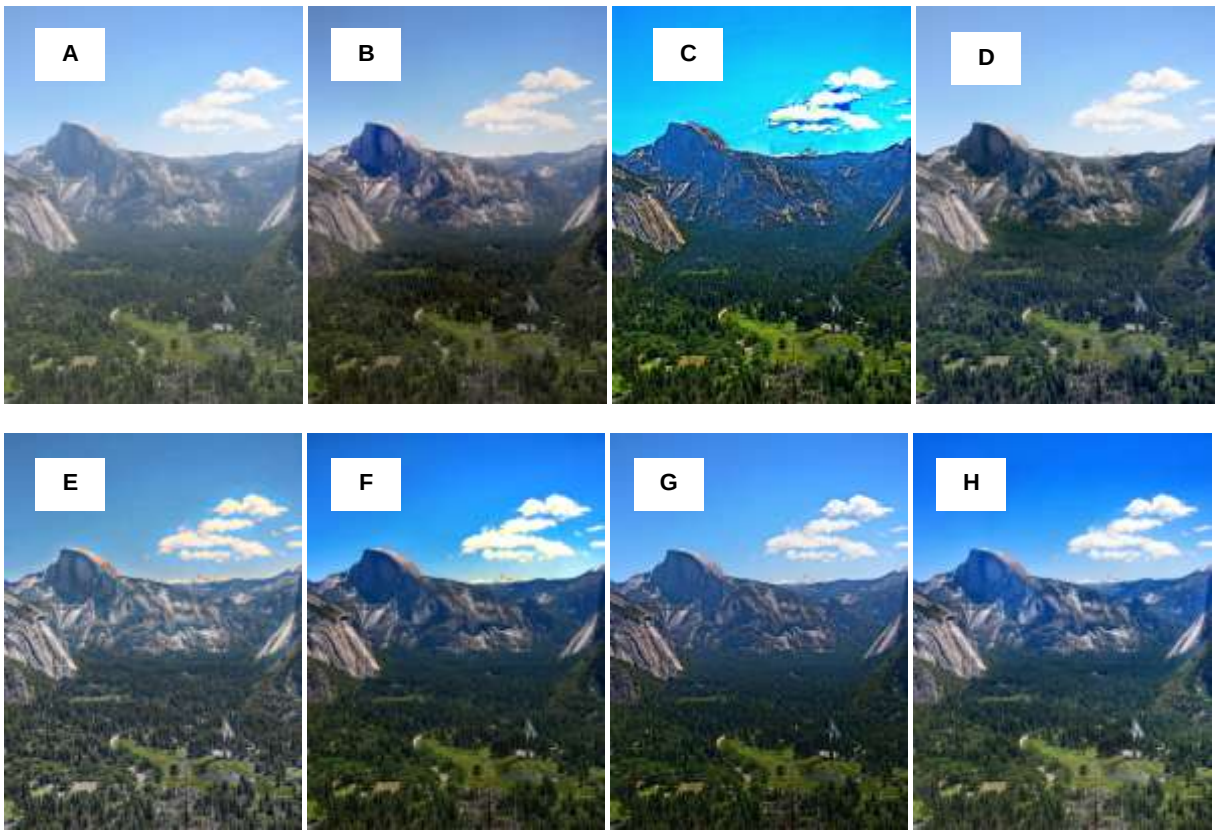

Figure 9: Comparison of qualitative performance with different algorithms of 'y01' (a) Original fogy image. (b) Fattal et al.'s method. (c) Tan et al.'s method. (d) Koef et al.'s method. (e) Tarel et al.'s method. (f)He et al.'s method. (g) A.K. et al.' method. (h) Presented method.

Figure 10: Comparison of qualitative performance with different algorithms of 'ny17' (a) Original fogy image. (b) Fattal et al.'s method. (c) Tan et al.'s method. (d) Koef et al.'s method. (e) Tarel et al.'s method. (f)He et al.'s method. (g) A.K. et al.' method. (h) Presented method.

Table 1: the presented algorithm and competition approaches.

Hazy image	**Y01**				**Y16**				**Ny17**			
Method	e	$\bar{r}$	Σ	C_{gain}	e	$\bar{r}$	Σ	C_{gain}	e	$\bar{r}$	Σ	C_{gain}
(Fattal, 2008)	0.0864	1.2152	0.0012	1.1540	0.0583	1.2033	0.0032	1.2458	-0.1061	1.5346	0.0202	1.4139
(Tan and Oakley, 2008)	0.1219	2.2283	0.0039	1.0209	-0.0165	2.0602	0.0045	0.9023	-0.0412	2.1900	0.0077	0.9101
(Kopf et al., 2008)	0.0947	1.6362	0.0002	1.3088	0.0009	1.3456	0.0028	1.3732	0.0169	1.6136	0.0136	1.5238
(Tarel and Hautiere, 2009)	0.2092	1.9903	0.0000	0.8272	0.2406	1.9583	0.0000	0.9218	0.1104	1.7057	0.0000	0.8375
(He et al., 2009)	0.1426	1.3134	0.0101	0.8688	0.1314	1.3674	0.0019	0.9052	0.0232	1.6297	0.0023	1.3204
Tripathi and Mukhopadhyay, 2012)	0.2532	1.4244	0.0000	1.0551	0.1632	1.4937	0.0002	0.9849	0.2456	2.1832	0.0036	1.4360
Proposed algorithm	0.1605	1.5955	0.0017	1.0879	0.1462	1.4015	0.0004	1.2635	0.0372	1.3173	0.0004	1.1157

Table 2: Mean opinion score (MOS) of different enhancement algorithms.

Quality vs Algorithms	**Color**	**Detail**	**Halo**	**Contrast**	**Natural**	**MOS**	**Score class**
(Fattal, 2008)	4.2	3.1	3.5	4.1	2.2	3.42	
(Tan and Oakley, 2008)	2.3	3.9	3.1	3.8	2.1	3.04	5 Excellent
(Kopf et al., 2008)	4.1	4.8	1.9	3.9	2.8	3.5	4 Good
(Tarel and Hautiere, 2009)	3.1	3.9	4.1	3.9	3.2	3.64	3 Fair
(He et al., 2009)	4.8	3.9	4.2	2.7	4.2	3.96	2 Poor
Tripathi and Mukhopadhyay, 2012)	3.4	3.6	3.1	3.0	3.2	3.26	1 Bad
Proposed algorithm	4.9	4.1	4.9	4.2	4.9	4.6	

algorithm can reveal more detailed information than that of He et al. (2009). The restored image appears joyful, which is like the texture of a stone. Objective indicators are compared with state-of-art algorithms in Table 1 to prove the advance of the presented approach.

MOS (Mean Opinion Score) is obtained by averaging the results of a set of standard and subjective tests. Twenty-two (22) volunteers rated the images enhanced by the methods discussed. Volunteers need to rate each image according to color constancy, fine details, halo artifacts, contrast perception, nature, and MOS performance. MOS is the arithmetic average of all individual scores, ranging from 1 (the worst) to 5 (the best).

Table 1 shows the results evaluated by four different indexes. Tan's and Tarel's methods have high values on e and $\bar{r}$, but its artifacts cannot be removed and the color distortion is serious. There are also some halos artifacts and color cast for other methods. The results indicate that the proposed algorithm show better balance performance for C_{gain}, Σ, and the gradient ratio $\bar{r}$. The proposed approach also results in a better balance performance for indicators, e.

Table 2 shows that the following conclusions can be drawn. The algorithm obtains a higher score in MOS. Therefore, even if our acquiring quality results are similar or little better than other approaches, the

visually dehazing effect seems much better because we get a better balance in term of contrast, edges and color. Furthermore, the proposed algorithm runs faster than others.

CONCLUSION

This paper discussed the atmosphere veil and illumination veil which are the decisive factors of image restoration in detail. The main contribution of this paper is to develop a unified dehazing method for blurred and non-illuminated images. Through the joint bilateral filtering, the method can achieve good color restoration even in severe grey environment. This reflects some basic schemes and principles of neuro computational awareness. It is helpful for the visual representation of illumination and color in optical imaging systems.

ACKNOWLEDGEMENTS

This work was supported by National Nature Science Foundation of China (NSFC) under Grants: 61671356, and 61201290.

REFERENCES

Ancuti C, Hermans C, Bekaert P (2011). A fast semi-inverse approach to detect and remove the haze from a single image, in: Proc. ACCV. pp. 501–514.

Asmuni H, Razib MO, Rohayanti H (2013). "An improved multiscale retinex algorithm for motion-blurred iris images to minimize the intra-individual variations. Pattern Recognition Letters. 34(9): 1071-1077.

Bai Y, Li C, Jia W, Li J, Mao Z-H, Sun M (2012). Designing a wearable computer for lifestyle evaluation". 38th Annual Northeast Bioengineering Conference; 2012 March 16-18; Philadelphia, PA. pp. 243-244.

Changhao S, Duan HB (2012). A restricted-direction target search approach based on coupled routing and optical sensor tasking optimization, OPTIK. 123(24)

Chao WH et al (2012). Correction of inhomogeneous magnetic resonance images using multiscale retinex for segmentation accuracy improvement. Biomedical Signal Processing and Control. 7(2): 129-140.

Dominik WA (2017). Exploiting the Redundancy of Multiple Overlapping Aerial Images for Dense Image Matching Based Digital Surface Model Generation. Remote Sens. 9:490.

Fattal R (2008). Single image dehazing. ACM Transactions on Graphics. 27(3): 1-9.

Garg K, Nayar SK (2007). Vision and rain. Int. J. Comput. Vis. 75(1), 3–27.

Hashemi S et al (2010). An image contrast enhancement method based on genetic algorithm. Pattern Recognition Letters. 31(13): 1816-1824.

Hautière N et al (2008). Blind contrast enhancement assessment by gradient ratioing at visible edges. Image Analysis Stereology Journal 27(2): 87-95.

He K, Jian S, Xiaoou T (2010). Guided image filtering. Computer Vision–ECCV 2010. Springer Berlin Heidelberg. pp.1-14.

He KM, Sun J,Tang X (2009). Single image haze removal using dark channel prior[C]. In: Proceedings of the IEEE Conference on Computer Vision and Pattern Recognition Miami. USA: IEEE. 1956-1963.

Huang SC, Yeh CH (2013). Image contrast enhancement for preserving mean brightness without losing image features. Engineering Applications of Artificial Intelligence. 26(5): 1487-1492.

Kim JH, Jang WD, Sim JY, et al (2013). Optimized contrast enhancement for real-time image and video dehazing. Journal of Visual Communication and Image Representation. 24(3): 410-425

Kopf J, Neubert B, Chen B, et al (2008). Deep photo: model-based photograph enhancement and viewing', ACM Trans. Graph. 27(5): 116:1–116:10

Li G, Li G, Han G (2017). Enhancement of Low Contrast Images Based on Effective Space Combined with Pixel Learning. Information. 8: 135.

Ma S, Ma H, Xu Y, Li S, Lv C, Zhu M (2018). A Low-Light Sensor Image Enhancement Algorithm Based on HSI Color Model. Sensors. 18: 3583.

Narasimhan SG, Nayar SK (2002). Vision and the atmosphere[J]. International Journal of Computer Vision. 48(3): 233-254.

Narasimhan SG, Nayar SK (2003). Contrast restoration of weather degraded images. IEEE Transactions on Pattern Analysis and Machine Intelligence. 25(6):713–724.

Paris S, Frédo D (2006). A fast approximation of the bilateral filter using a signal processing approach. Computer Vision–ECCV 2006. Springer Berlin Heidelberg. pp. 568-580.

Rahman, Zia-ur, Daniel J. Jobson, Glenn A (2004). Woodell. "Retinex processing for automatic image enhancement. Journal of Electronic Imaging13(1):100-110.

Schechner YY, Narasimhan SG, Nayar SK (2003). Polarization-based vision through haze. Applied Optics. 42(3): 511-525.

Seo DK, Kim YH, Eo YD, Park WY (2018). Learning-Based Colorization of Grayscale Aerial Images Using Random Forest Regression. Appl. Sci. 2018, 8, 1269.

Sun W, Long H, Baolong G, Wenyan J, Mingui S (2014). A fast color image enhancement algorithm based on Max Intensity Channel. Journal of Modern Optics 61(6): 466-477.

Tan K, Oakley PJ (2001). Physics-based approach to color image enhancement in poor visibility conditions [J]. Optical Society of America. 18(10): 2460-2467.

Tan R (2008). Visibility in bad weather from a single image. In IEEE Conference on Computer Vision and Pattern Recognition (CVPR'08), pp. 1–8.

Tarel JP, Hautiere N (2009). Fast visibility restoration from a single color or gray level image. In: Proceedings of the 12th IEEE International Conference on Computer Vision Kyoto.Japan: IEEE. pp.2201-2208.

Tripathi AK, Mukhopadhyay S (2012). Single Image Fog Removal Using Anisotropic Diffusion", IET Image processing. 6(7): 966 – 975.

Wei S (2013). A New Single Image Fog Removal Algorithm Based on Physical Model, International Journal for Light and Electron Optics. 124(21): 4770-4775.

Wei S, Guo B (2013). A fast single-image dehazing method for visible-light systems,Optical Engineering. 52(9): 093-103

Xiao C, Gan J (2012). Fast image dehazing using guided joint bilateral filter. The Visual Computer. 28(6-8): 713-721.

Ye X, Wu G, Huang L, Fan F, Zhang Y (2018). Image Enhancement for Inspection of Cable Images Based on Retinex Theory and Fuzzy Enhancement Method in Wavelet Domain. Symmetry. 10: 570.

Yeh CH, Kang LW, Lee MS, Lin, CY (2013). Haze effect removal from image via haze density estimation in optical model. Optics express, 21(22), 27127-27141.

Zhang B, Jan P (2008). Allebach.Adaptive bilateral filter for sharpness enhancement and noise removal. Image Processing, IEEE Transactions. 17(5): 664-678.